euronoise 2021
25th to 27th of October
Madeira, Portugal - online

A modal transfer matrix approach for the prediction of impact sound insulation

J. Vastiau, C. Van hoorickx, E. Reynders

KU Leuven, Department of Civil Engineering
Kasteelpark Arenberg 40, 3001, Leuven, Belgium
{jasper.vastiau@kuleuven.be}

Abstract
Wave propagation in layered media of fluid, elastic and porous nature is commonly analyzed with the transfer matrix method (TMM). Up to now it has been used extensively to analyze airborne sound transmission and sound absorption. Its use for impact sound transmission has been investigated to a limited extent, i.e. for infinite thick homogeneous elastic plates and for specific receiver locations. This contribution aims to broaden the scope such that the impact sound power radiated by finite floors containing elastic, fluid and/or porous layers, can be accurately analyzed. A disadvantage of the conventional TMM is that only floors of infinite extent can be implemented. In order to approximately model finite floors with simply supported boundary conditions, the vibration field of the floor is expressed in terms of sinusoidal lateral basis functions, which relate to the traveling waves that are analyzed with the TMM. The resulting approach is termed the modal TMM, or mTMM. A standard tapping machine provides the structural excitation and all five hammers are taken into account for a more accurate representation of the excitation force, with respect to the common simplification where only one hammer is modelled. Predictions of the radiated sound power are validated with measurements for a bare floor and a floating floor.

Keywords: transfer matrix, impact sound, standard tapping machine.

1 Introduction

The transfer matrix method (TMM) [1-5] is widely used to predict the airborne sound insulation and sound absorption of layered wall and floor systems. An advantage of the method is that different types of layer can be incorporated such as fluid, solid and porous layers. Accurate results of the sound insulation are achieved at high frequencies. The method has been used only to a limited extent for the prediction of impact sound radiation of a homogeneous single layered floor [6]. However, some drawbacks are related to this method. First, an empiric expression is proposed in [6] to compute the sound pressure level in the receiver room. Second, the floors are of infinite extent. Third, the result is not accurate at low frequencies because the boundary conditions and resulting modal behavior of the floor are neglected. A previous extension to the methodology has been published, where the radiated sound power level is computed in the spatial domain [7] or wavenumber domain [8,9] for infinite multilayered floors. However, this method still neglects the finite floor size and its modal behavior. Spatial windowing techniques [10,11] have been developed to account for the finite floor size. However, these techniques still omit the modal behavior of the floor. As an improvement on the state of the art, the modal TMM (mTMM) [12] is adopted to compute the sound power radiated from finite floors, while also accounting for the modal behavior of the floor.

A standard tapping machine, for which the properties are prescribed in ISO 10140-5 [13], is used to provide an excitation force to the floor. A tapping machine consists of five hammers, impacting consecutively every 0.1s. In literature, the simplification is often made that only one hammer impacts on the floor every 0.1 s [8,14,15]. This assumption causes the spectral shape of the emitted sound to be a 10 Hz line spectrum, whereas a narrowband measurement of a timber joist floor excited by a standard tapping machine revealed a 2 Hz line spectrum [16]. This contribution takes all five impact hammers into account, including the time delay between hammer impacts, as well as the difference in location and driving point admittance due to the hammer spacing in order to accurately predict the excitation force of the standard tapping machine.

The remainder of this paper is organized as follows. The prediction method for the radiated sound power of finite floors using the mTMM in the wavenumber domain is presented in section 2. Validation examples for the radiated sound power from multilayer floors are discussed in section 3. Concluding remarks are given in section 4.

2 Prediction method

In the first step of the prediction method, the mathematical description of the force exerted on the floor by a standard tapping machine is introduced. All five hammers are considered to construct a correct force signal. In a second step, the velocity field at the lower side of the floor is obtained as a result of wave propagation through the floor, which is modelled using the mTMM. In the third step, a relation is obtained between the external force and the pressure field at the floor surface. In the fourth and last step, the velocity field at the lower side of the floor is used to compute the radiated sound power into the receiver room, assuming a weak coupling of the floor and the air volume in the receiver room.

2.1 Impact force

All results are based on mechanical excitation of the floor by means of a standard tapping machine, which produces a periodic impact force, assumed to be of very short duration at t = 0 for hammer 1. This periodic impact force of hammer 1 can be represented by an exponential form of the Fourier series [3,17].

$$F^{(1)}(t) = \sum_{n=-\infty}^{\infty} F_n^{(1)} \, \mathrm{e}^{i\frac{2\pi n}{T}t} = F_0^{(1)} + 2\sum_{n=1}^{\infty} F_n^{(1)} \cos\left(\frac{2\pi n}{T}t\right) \tag{1}$$

with $\omega_0 = \frac{2\pi}{T}$, $F_n^{(1)} = \frac{1}{T}\int_0^T F^{(1)}(t)\mathrm{e}^{-i\frac{2\pi n}{T}t}dt$

where $F_n^{(1)}$ represents the amplitude of the nth harmonic component of the impact force resulting from hammer 1. For a standard tapping machine, each hammer has a mass of m = 0.5 kg and has a free-drop height of h = 0.04 m, as specified by ISO 10140-5:2010 [1]. Since the duration of the force pulse is short with respect to the period of interest, the Fourier amplitude of the harmonics can be approximated by $e^{-i\frac{2\pi n}{T}t} \approx 1$ [4,17]. Considering the contribution of each impact hammer separately, the period of the hammers equals T=0.5 s. The impulse-momentum theorem [18] is used to express the Fourier coefficients in terms of the known mass and drop height of the hammers, assuming ideal elastic impacts to obtain an upper limit for the force amplitude.

$$F_n^{(1)} \approx \frac{1}{T}\int_0^T F^{(1)}(t)dt = \frac{2mv_0}{T} = \frac{2m}{T}\sqrt{2gh} = 1.77\ N \tag{2}$$

The time-signal of the kth hammer displays a delay t_k of the impact time with respect to the first hammer at t = 0 s. The order of impacts from the hammers is 1-3-5-2-4, with an interval of 0.1 s between each hammer.

$$F^{(k)}(t-t_k) = \sum_{n=-\infty}^{\infty} F_n^{(k)} e^{i\frac{2\pi n}{T}(t-t_k)} \tag{3}$$

Which constitutes a phase angle $-\frac{2\pi n}{T}t_k$ for the n[th] harmonic of hammer k. The phase shifts of all hammers are visualized in Figure 1, showing that the forces always cancel each other out, except at 10 Hz multiples where all hammers act in phase. Of course this conclusion only holds under the assumption that all hammers hit the structure at the exact same location. If the distance between the hammers is accounted for, the force amplitudes will vary due to the fact that the floor has a location dependent point mobility, such that the phases will no longer cancel out the hammer forces entirely and sound radiation at 2 Hz multiples will occur.

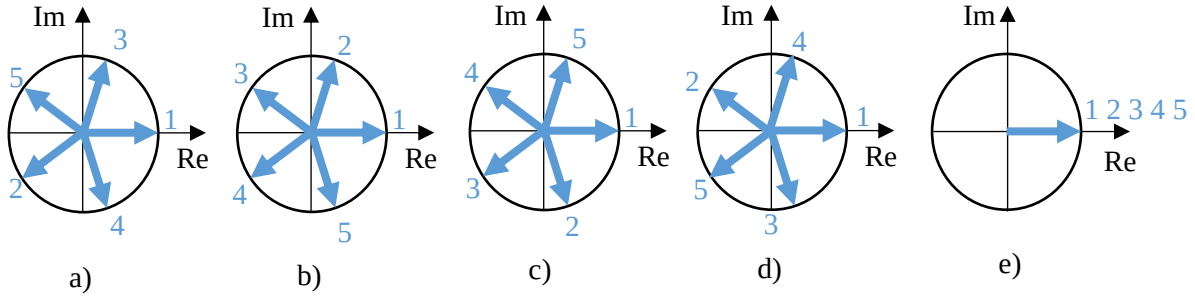

Figure 1: Phase shift for each of the five hammers a) 1[st] harmonic (2 Hz) b) 2[nd] harmonic (4 Hz) c) 3[rd] harmonic (6 Hz) d) 4[th] harmonic (8 Hz) e) 5[th] harmonic (10 Hz).

2.2 Velocity field

For homogeneous elastic solid layers in the TMM, as illustrated in Figure 2, the acoustic state is represented by four variables in the frequency-wavenumber domain: the velocity in x-direction v_x^s and z-direction v_z^s, the normal stress in the vertical direction σ_{zz} and the shear stress σ_{xz}. This acoustic state is represented by the vector $V^s(M)$, where the superscript s denotes a solid layer. Note that these four variables are sufficient to completely describe the deformation and stress state of the layer as the TMM considers two-dimensional wave propagation in the xz-plane. The states on the top side ($z = \mathrm{z_A}$) and bottom side ($z = \mathrm{z_B}$) of a homogeneous elastic layer are related through a transfer matrix T^s [6,10,19]. z_A denotes the side where the impact force is applied, while z_B denotes the floor-receiver room interface. The elements of the transfer matrix as well as the acoustic state variables depend on the trace wavenumber $k_r = \sqrt{k_x^2 + k_y^2}$

$$\boldsymbol{V}^s(k_r, \omega, \mathrm{z_A}) = [v_x^s(k_r, \omega, \mathrm{z_A})\ \ v_z^s(k_r, \omega, \mathrm{z_A})\ \ \sigma_x^s(k_r, \omega, \mathrm{z_A})\ \ \sigma_x^s(k_r, \omega, \mathrm{z_A})]^T \tag{4}$$

$$\boldsymbol{V}^s(k_r, \omega, \mathrm{z_A}) = \boldsymbol{T}^s(k_r, \omega)\boldsymbol{V}^s(k_r, \omega, \mathrm{z_B}) \tag{5}$$

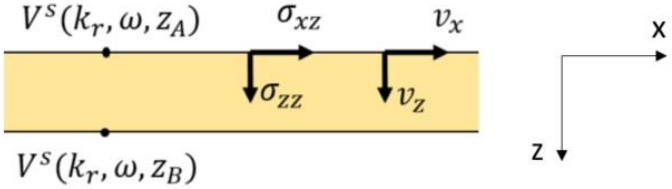

Figure 2: Convention used in the mTMM model, with the receiver room at positive z-coordinates.

In case of a bare floor, only a single elastic layer is present. When considering a vertical impact force on the floor, 4 boundary conditions are needed to solve the wave field. The vertical stress at the impact side equals $\sigma_{zz}(k_r, \omega, \mathrm{z_A})$ and will further on be related to the external force. There is no shear stress at either side of the floor, i.e. $\sigma_{xz}(k_r, \omega, \mathrm{z_A}) = \sigma_{xz}(k_r, \omega, \mathrm{z_B}) = 0$. The vertical stress at the receiver room interface is approximately zero when weak coupling is assumed between the floor and the air volume, so $\sigma_{zz}(k_r, \omega, \mathrm{z_B}) \approx 0$. These boundary conditions lead to four known stresses, so only the velocities of the acoustic states at both floor edges are unknown. They are described by following vectors:

$$\boldsymbol{V}^s(k_r, \omega, \mathrm{z_A}) = [v_x^s(k_r, \omega, \mathrm{z_A})\ \ v_z^s(k_r, \omega, \mathrm{z_A})\ \ \sigma_{zz}(k_r, \omega, \mathrm{z_A})\ 0]^T \tag{6}$$

$$\boldsymbol{V}^s(k_r, \omega, \mathrm{z_B}) = [v_x^s(k_r, \omega, \mathrm{z_B})\ \ v_z^s(k_r, \omega, \mathrm{z_B})\ \ 0\ 0]^T \tag{7}$$

For thick, finite floors, the velocity field can be approximated using a Ritz approach, i.e. by means of a generalized velocity $v_j(z, \omega)$ and a finite set of shape functions $\phi(x, y)$ that satisfy the simply supported boundary conditions at any coordinate z.

$$v(x, y, z, \omega) = \sum_{j=1}^{N_m} v_j(z, \omega)\phi_j(x, y) \tag{8}$$

For finite floors the origin of the coordinate system is located at a corner of the floor for computational purposes, so coordinates range from $[0\,;0]$ to $[L_x\,;L_y]$. The floor is assumed to have a rectangular shape, composed of homogeneous layers with simply supported boundary conditions and hysteretic damping. The chosen shape functions are mass normalized sine functions [2].

$$\phi_j(x, y) = \frac{2}{\sqrt{\rho t L_x L_y}} \sin\left(\frac{m_j \pi}{L_x} x\right) \sin\left(\frac{m_j \pi}{L_y} y\right) \tag{9}$$

where $\frac{m_j \pi}{L_x} = k_{jx}$ and $\frac{n_j \pi}{L_y} = k_{jy}$ are the x and y components of the modal wavenumber, ρ is the mass density, t is the floor thickness and m_j and n_j are the number of half wavelengths of mode j in the x and y directions, respectively.

The transfer matrix relates the acoustic states of the top and bottom sides of the floor. Equation 5 can be reformulated [13] such that a mechanical impedance matrix relates the velocities at both sides of the floor to the stresses at both sides of the floor. This mechanical impedance formulation is repeated for the Cartesian wavenumber domain, where the decomposition of the velocity field (cfr. Equation 8) is performed and where the trace wavenumber, imposed on the TMM, is the modal wavenumber $k_j = \sqrt{k_{jx}^2 + k_{jy}^2}$.

$$\sum_{j=1}^{N_m} \left(Z_{AA}(k_j, \omega) v_j(\mathrm{z_A}, \omega) + Z_{AB}(k_j, \omega) v_j(\mathrm{z_B}, \omega) \right) \phi_j(x, y) = p(x, y, \mathrm{z_A}, \omega) \tag{10}$$

$$\sum_{j=1}^{N_m} \left(Z_{BA}(k_j, \omega) v_j(\mathrm{z_A}, \omega) + Z_{BB}(k_j, \omega) v_j(\mathrm{z_B}, \omega) \right) \phi_j(x, y) = p(x, y, \mathrm{z_B}, \omega) \tag{11}$$

A weighted residual formulation is then constructed with weight function $\phi_l(x, y)$.

$$\begin{cases} \int_0^{L_x}\int_0^{L_y}\left[\sum_{j=1}^{N_m}\left(Z_{AA}(k_j,\omega)v_j(\mathrm{z_A},\omega)+Z_{AB}(k_j,\omega)v_j(\mathrm{z_B},\omega)\right)\phi_j(x,y)\right]\phi_l(x,y)\mathrm{d}x\mathrm{d}y \\ \qquad = \int_0^{L_x}\int_0^{L_y} p(x,y,\mathrm{z_A},\omega)\,\phi_l(x,y)\mathrm{d}x\mathrm{d}y \\ \int_0^{L_x}\int_0^{L_y}\left[\sum_{j=1}^{N_m}\left(Z_{BA}(k_j,\omega)v_j(\mathrm{z_A},\omega)+Z_{BB}(k_j,\omega)v_j(\mathrm{z_B},\omega)\right)\phi_j(x,y)\right]\phi_l(x,y)\mathrm{d}x\mathrm{d}y \\ \qquad = \int_0^{L_x}\int_0^{L_y} p(x,y,\mathrm{z_B},\omega)\,\phi_l(x,y)\mathrm{d}x\mathrm{d}y \end{cases} \tag{12}$$

The shape functions $\phi_j(x,y)$ are orthogonal to each other, so the following equation is valid:

$$\int_0^{L_x}\int_0^{L_y}\phi_l(x,y)\,\phi_j(x,y)\mathrm{d}x\mathrm{d}y = \frac{1}{\rho t}\delta_{jl} \tag{13}$$

Substituting the decomposition from Equation 8 into the mechanical impedance expression of Equations 10 and 11, leads to following relation between the generalized velocities and pressures for a single mode j.

$$\begin{bmatrix} Z_{AA}^{S}(k_j,\omega) & Z_{AB}^{S}(k_j,\omega) \\ Z_{BA}^{S}(k_j,\omega) & Z_{BB}^{S}(k_j,\omega) \end{bmatrix}\begin{bmatrix} v_j(\mathrm{z_A},\omega) \\ v_j(\mathrm{z_B},\omega) \end{bmatrix} = \begin{bmatrix} p_j(\mathrm{z_A},\omega) \\ p_j(\mathrm{z_B},\omega) \end{bmatrix} \tag{14}$$

The resulting velocity field is finally transformed to the wavenumber domain, where the integration bounds are limited since the shape functions are equal to zero beyond the edges of the floor surface and this integral can be solved analytically. Incorporation of the approximate modal behavior of finite floors requires computation of the resulting velocity field in the (k_x,k_y) wavenumber domain, in contrast to infinite floors where the cylindrical wavenumber domain is preferred due to the axisymmetric nature of the wave propagation.

$$\begin{aligned} v(k_x,k_y,z,\omega) &= \int_0^{L_x}\int_0^{L_y} v(x,y,z,\omega)e^{\mathrm{i}k_x x}e^{\mathrm{i}k_y y}\mathrm{d}x\mathrm{d}y \\ &= \sum_{j=1}^{N_m} v_j(z,\omega)\int_0^{L_x}\int_0^{L_y}\phi_j(x,y)e^{\mathrm{i}k_x x}e^{\mathrm{i}k_y y}\mathrm{d}x\mathrm{d}y \\ = \frac{2}{\sqrt{\rho t L_x L_y}}\sum_{j=1}^{N_m} v_j(z,\omega)&\left(\frac{k_{jx}\left(1-(-1)^{m_j}e^{ik_x L_x}\right)}{\left(k_{jx}^2-k_x^2\right)}\right)\left(\frac{k_{jy}\left(1-(-1)^{n_j}e^{ik_y L_y}\right)}{\left(k_{jy}^2-k_y^2\right)}\right) \end{aligned} \tag{15}$$

2.3 Relation between external force and floor surface pressure

The external point force can be expressed as an integration of the pressure field over the floor surface.

$$F(\omega) = \int_0^{L_x}\int_0^{L_y} p(x,y,\mathrm{z_A},\omega)dxdy \tag{16}$$

Where

$$p(x,y,\mathrm{z_A},\omega) = F(\omega)\delta(x)\delta(y) \tag{17}$$

To determine the generalized pressure at the impact side ($z = z_A$), an expression is required to relate the generalized pressure to the impact force $F(\omega)$.

$$\int_0^{L_x}\int_0^{L_y} \phi_l(x,y)\, p(x,y,\mathrm{z_A},\omega)\mathrm{d}x\mathrm{d}y = \sum_{j=1}^{N_m}\int_0^{L_x}\int_0^{L_y} \phi_l(x,y)\, \phi_j(x,y) p_j(\mathrm{z_A},\omega)\mathrm{d}x\mathrm{d}y \tag{18}$$

Using the orthogonality from Equation 13 in Equation 18 results in

$$\int_0^{L_x}\int_0^{L_y} \phi_l(x,y)\, p(x,y,\mathrm{z_A},\omega)\mathrm{d}x\mathrm{d}y = \sum_{J=1}^{N_m}\frac{1}{\rho t}\delta_{jl} p_j(\mathrm{z_A},\omega) \tag{19}$$

and subsequent substitution of Equation 17 into above expression yields a relation between the generalized pressure and the impact force.

$$p_j(\mathrm{z_A},\omega) = \rho t \phi_j(x_f,y_f) F(\omega) \tag{20}$$

2.4 Radiated sound power

The room is modelled as an acoustic halfspace, so the sound is radiated by the floor into the direct field of the room. The relation between pressure and velocity at the floor-room interface depends on the ratio of the trace wavenumber $\sqrt{k_x^2 + k_y^2}$ and the wavenumber in air k_a [2].

$$\begin{cases} p\big(k_x,k_y,z,\omega\big) = \rho_a c \dfrac{k_a(\omega)}{\sqrt{k_a^2(\omega) - \big(k_x^2+k_y^2\big)}} v\big(k_x,k_y,z,\omega\big) & k_x^2 + k_y^2 \le k_a^2(\omega) \\ p\big(k_x,k_y,z,\omega\big) = \rho_a c \dfrac{k_a(\omega)}{-\mathrm{i}\sqrt{\big(k_x^2+k_y^2\big) - k_a^2(\omega)}} v\big(k_x,k_y,z,\omega\big) & k_x^2 + k_y^2 \ge k_a^2(\omega) \end{cases} \tag{21}$$

The radiated sound power W is obtained in the spatial domain by integration of the sound intensity over the entire floor surface. To this end, a double inverse wavenumber transform is applied to the velocity and pressure at the floor-room interface.

$$p(x,y,z,\omega) = \frac{1}{4\pi^2}\int_{-\infty}^{\infty}\int_{-\infty}^{\infty} p\big(k_x,k_y,z,\omega\big) e^{-\mathrm{i}k_x x} e^{-\mathrm{i}k_y y}\mathrm{d}k_x\mathrm{d}k_y \tag{22}$$

$$v(x,y,z,\omega) = \frac{1}{4\pi^2}\int_{-\infty}^{\infty}\int_{-\infty}^{\infty} v\big(k'_x,k'_y,z,\omega\big) e^{-\mathrm{i}k'_x x} e^{-\mathrm{i}k'_y y}\mathrm{d}k'_x\mathrm{d}k'_y \tag{23}$$

The use of k and k' is introduced to make a clear distinction between both integral variables. The sound power is expressed as

$$W(\omega) = \frac{1}{2}\mathrm{Re}\left(\int_0^{L_x}\int_0^{L_y} p(x,y,\mathrm{z_B},\omega) v^*(x,y,\mathrm{z_B},\omega)\mathrm{d}x\mathrm{d}y\right) \tag{24}$$

The integration boundaries can be extended from $[0\,;L_x]$ and $[0\,;L_y]$ to $]-\infty\,;\infty[$ as the shape functions are equal to zero outside of the floor surface area and consequently there is no sound power radiation beyond the floor boundaries. Substitution of Equations 22 and 23 into Equation 24 and subsequent integrations over (x,y) and $(k'_x\,,k'_y)$ [20] lead to following expression for the sound power radiation in the wavenumber domain:

$$W(\omega) = \frac{1}{8\pi^2}\mathrm{Re}\left(\int_{-\infty}^{\infty}\int_{-\infty}^{\infty} p(k_x, k_y, z_B, \omega) v^*(k_x, k_y, z_B, \omega) \mathrm{d}k_x \mathrm{d}k_y\right) \quad (25)$$

This is a double infinite integral. However, only wavenumber components satisfying the condition $k_x^2 + k_y^2 \leq k_a^2(\omega)$ contribute to the real part of the integral and thus to net sound power radiation, such that the range of integration can be reduced. Substituting the first expression of Equation 21 into the reduced integral leads to a compact formulation for the radiated sound power. This expression can be simplified due to the quadratic nature of the integrand, leading to a significant increase in computational efficiency.

$$W(\omega) = \frac{\rho_a c k_a(\omega)}{2\pi^2}\mathrm{Re}\left(\int_0^{k_a(\omega)}\int_0^{\sqrt{k_a(\omega)^2 - k_y^2}} \frac{\left|v(k_x, k_y, z_B, \omega)\right|^2}{\sqrt{k_a(\omega)^2 - (k_x^2 + k_y^2)}} \mathrm{d}k_x \mathrm{d}k_y\right) \quad (26)$$

3 Validation

A validation case is included for the analysis of a multilayered structure. Measurements were performed by the BBRI [21] on a floating floor with horizontal dimensions $L_x = 2.60$ m and $L_y = 4.42$ m. The floor was impacted with a standardized tapping machine. Measurements were performed for at least four unknown impact locations. The results for the prediction models in Figure 3 are an average of the results from four randomly distributed impact locations at (0.75 m, 1.02 m); (2.06 m, 2.03 m); (1.32 m, 3.78 m) and at (1.72 m, 2.94 m) for the middle hammer, where it is assumed that the tapping machine was placed along the y-axis. All relevant layer properties are provided in Table 1. Measurement results for the bare concrete floor and the floating floor system are illustrated in Figure 3: as well as predictions for the radiated sound power using two models for the impact force: a model where one force impacts at 10 Hz and a model where all five hammers at 2 Hz are included and the distance between hammers is accounted for. Measurement results were obtained down to the 50 Hz one-third octave band. It is clear from the figure that the one hammer model and the five hammer model yield nearly identical results at 50 Hz and above. The single number ratings $L_{n,W}(C_I)$ for the measurements are 68 dB (+0 dB) for the bare floor and 36 dB (+13 dB) for the floating floor, while both prediction methods have an identical SNR, which is 70 dB (-4 dB) for the bare floor and 36 dB (+11 dB) for the floating floor.

Table 1: Layering and material properties of the floating floor. * Assumed values which are widely used in literature. ** Estimated properties.

Layer	$\rho\ [kg/m^3]$	$t\ [m]$	$\eta\ [-]$	$\nu\ [-]$	$E\ [N/m^2]$
Floating screed	1800	0.06	0.015 *	0.2 *	31.5e9(1+ηi) *
INSULIT BI+8	40	0.008	0.8 **	0.3 **	1.6e5(1+ηi) *
Base concrete floor	2400	0.14	0.015 *	0.2 *	31.5e9(1+ηi) *

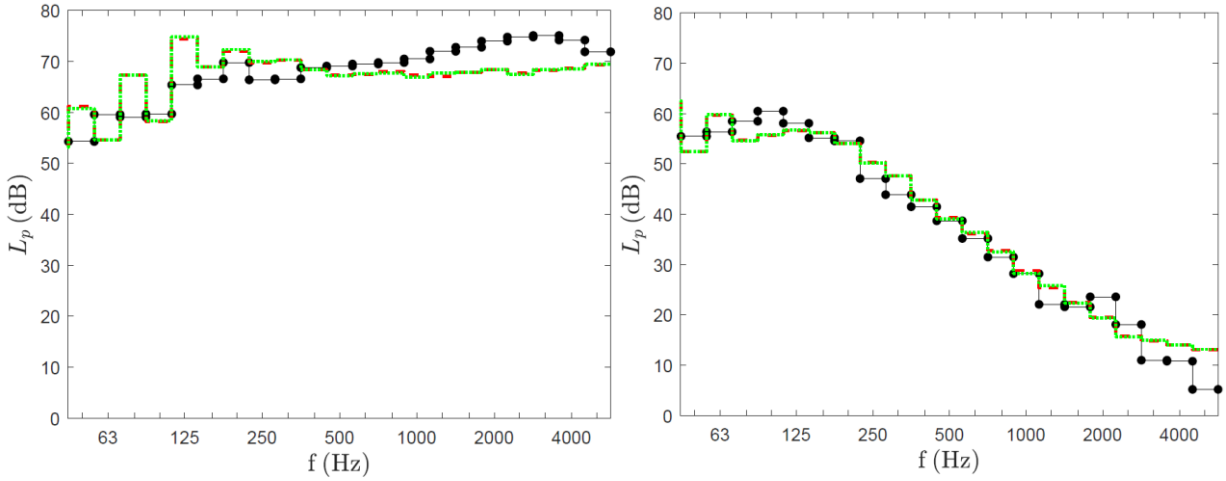

(a) (b)

Figure 3: Radiated sound pressure level: measurement (black), 5 hammer prediction (red dashed line) 1 hammer prediction (green dotted line) for (a) bare concrete floor (b) floating floor

In Figure 4, the prediction method is extended down to the 6.3 Hz one-third octave band. As a reference solution, a prediction of the radiated sound pressure level using an averaged force spectrum [13] is shown. It is clear that the assumption of 1 hammer acting at 10 Hz is valid from 40 Hz onward, but for lower bands, there would be no or only one line present in the force spectrum, leading to a high uncertainty or even no radiated power at all. The results for the prediction model using five hammers still displays distinct peaks at 10 Hz multiples since all hammers act in phase, but the harmonic results clearly show that the sound pressure level is nonzero at 2 Hz multiples, because the difference in location of the hammers yields different amplitudes for the hammer forces an consequently they don't cancel out anymore due to their phase differences. The 10 Hz multiples still dominate the resulting spectrum, as the difference between the 10 Hz multiples and the 2 Hz multiples is around 25 dB.

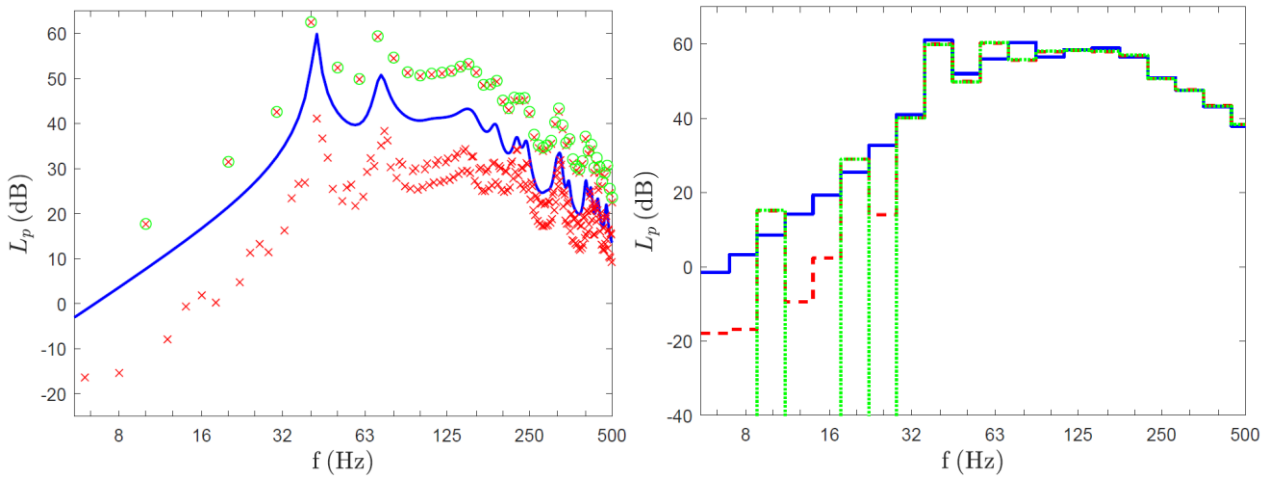

(a) (b)

Figure 4: Radiated sound power level, computed with an averaged force spectrum [13] (blue solid line), 1 hammer acting at 10 Hz (green) and the 5 hammers acting at 2 Hz (red) (a) harmonic sound power level (b) sound power level in one-third octave bands.

4 Conclusions

The mTMM framework is presented for finite floors. Validation examples have shown that the mTMM has an accuracy of a few dB for the entire 50-5000 Hz frequency range, since the boundary conditions and resulting modal behavior are accounted for. It has been shown that when analyzing a structure below 50 Hz, it is important to use a more detailed mathematical formulation for the impact force, taking into account all five hammers acting at 2 Hz and the distance between those hammers.

Acknowledgements

This research was funded by the European Research Council (ERC) Executive Agency, in the form of an ERC Starting Grant provided to Edwin Reynders under the Horizon 2020 framework program, project 714591 VirBAcous. The financial support from the European Commission is gratefully acknowledged.

References

[1] W.T. Thomson. Transmission of elastic waves through a stratified solid medium. *Journal of Applied Physics*, 21:89–93, 1950.
[2] W. Lauriks, P. Mees, and J. F. Allard. The acoustic transmission through layered systems. *Journal of Sound and Vibration*, 155(1):125–132, 1992.
[3] B. Brouard, D. Lafarge, and J.F. Allard. A general method of modelling sound propagation in layered media. *Journal of Sound and Vibration*, 183(1):129–142, 1995.
[4] J.-F. Allard and N. Atalla. *Propagation of sound in porous media*. John Wiley & Sons, Chichester, UK, 2nd edition, 2009.
[5] N. Geebelen. *Structure-borne sound sensitivity of building structures: assessment of the acoustic performances of multilayered structures by simulation and measurement techniques*. PhD thesis, Department of Civil Engineering, KU Leuven, 2008.
[6] A Tadeu, A Pereira, L Godinho, and J Antonio. Prediction of airborne sound and impact sound insulation provided by single and multilayer systems using analytical expressions. *Applied Acoustics*, 68(1):17–42, 2007.
[7] J. Vastiau, C. Decraene, C. Van hoorickx, and E.P.B. Reynders. Impact sound prediction of multilayered structures with the (modal) transfer matrix method. *In Proceedings of the 29th International Conference on Noise and Vibration Engineering*, ISMA 2020, Leuven, Belgium, September 2020.
[8] L. Cremer and M. Heckl. *Structure-borne sound: Structural vibrations and sound radiation at audio frequencies*. Springer, Berlin, 2nd edition, 1988.
[9] J. Vastiau, C. Van hoorickx, and E.P.B. Reynders. Wavenumber domain solution for impact sound prediction of finite floors with the (modal) transfer matrix method. In *Proceedings of the 50th International Congress and Exposition on Noise Control Engineering, Inter-Noise 2021*, Washington D.C., August 2021. Paper submitted.
[10] M. Villot, C. Guigou, and L. Gagliardini. Predicting the acoustical radiation of finite size multi-layered structures by applying spatial windowing on infinite structures. *Journal of Sound and Vibration*, 245(3):433–455, 2001.
[11] T.E. Vigran. Predicting the sound reduction index of finite size specimen by a simplified spatial windowing technique. *Journal of Sound and Vibration*, 325(3):507–512, 2009.
[12] C. Decraene, A. Dijckmans, and E.P.B. Reynders. Fast mean and variance computation of the diffuse sound transmission through finite-sized thick and layered wall and floor systems. *Journal of Sound and Vibration*, 422:131–145, 2018.
[13] International Organization for Standardization. ISO 10140-5: *Acoustics – Laboratory measurement of sound insulation of building elements – Part 5: Requirements for test facilities and equipment*, 2010.

[14] I.L. Vér. Impact noise isolation of composite floors. *Journal of the Acoustical Society of America*, 50(4):1043–1050, 1971.
[15] J. Brunskog and P. Hammer. The interaction between the ISO tapping machine and lightweight floors. *Acta Acustica united with Acustica*, 89(2):296-308, 2003.
[16] V. Wittstock. On the spectral shape of the sound generated by standard tapping machines. *Acta Acustica united with Acustica*, 98:301-308, 2012.
[17] A. Rabold, M. Buchschmid, A. Düster, G. Müller, and E. Rank. Modelling the excitation force of a standard tapping machine on lightweight floor structures. *Building Acoustics*, 17(3):175-197, 2010.
[18] Nihat Özkaya, Dawn Leger, David Goldsheyder, and Margareta Nordin. *Impulse and momentum*, pages 253–278. Springer, 2017.
[19] D.L. Folds and C.D. Loggins. Transmission and reflection of ultrasonic waves in layered media. *Journal of the Acoustical Society of America*, 62(5):1102–1109, 1977.
[20] F. Fahy and P. Gardonio. *Sound and structural vibration: radiation, transmission and response*. Academic Press, Oxford, UK, 2nd edition, 2007.
[21] Belgian Building Research Institute. *Proefverslag AC7718*, 2017.